

1 **Main Manuscript for**

2 **Single-cell RNA-seq analysis reveals penaeid shrimp hemocyte**  
3 **subpopulations and cell differentiation process**

4 Keiichiro Koiwai <sup>a, \*</sup>, Takashi Koyama <sup>b, c</sup>, Soichiro Tsuda <sup>d</sup>, Atsushi Toyoda <sup>e</sup>, Kiyoshi Kikuchi <sup>b</sup>,  
5 Hiroaki Suzuki <sup>f</sup>, Ryuji Kawano <sup>a</sup>

6 <sup>a</sup> Department of Biotechnology and Life Science, Tokyo University of Agriculture and Technology,  
7 Koganei-shi, Tokyo 184-8588, Japan

8 <sup>b</sup> Fisheries Laboratory, Graduate School of Agricultural and Life Sciences, The University of Tokyo,  
9 Hamamatsu, Shizuoka 431-0214, Japan

10 <sup>c</sup> Graduate School of Fisheries and Environmental Sciences, Nagasaki University, Bunkyo-machi,  
11 Nagasaki-shi, Nagasaki 852-8521, Japan

12 <sup>d</sup> bitBiome Inc., Waseda University Incubation Center, Nishiwaseda, Shinjuku-ku, Tokyo 169-0051,  
13 Japan

14 <sup>e</sup> Advanced Genomics Center, National Institute of Genetics, Mishima, Shizuoka 411-8540, Japan

15 <sup>f</sup> Department of Precision Mechanics, Faculty of Science and Engineering, Chuo University,  
16 Bunkyo-ku, Tokyo 112-8551, Japan

17 \* Keiichiro Koiwai

18 **Email:** [koiwai@go.tuat.ac.jp](mailto:koiwai@go.tuat.ac.jp)

19 **Author Contributions:** K. Koiwai designed the experiments; K. Koiwai, T.K., S.T., and A.T.  
20 performed the experiments; K. Koiwai analyzed the data; K. Kikuchi, H.S., and R.K. supervised the  
21 research; K. K. wrote the paper.

22 **Competing Interest Statement:** The authors declare no conflict of interest.

23 **Classification:** Agricultural Sciences

24 **Keywords:** scRNA-seq; non-model; hemocytes; cell differentiation; crustacean; shrimp

25 **This PDF file includes:**

26 Main Text

27 Figures 1 to 7

## 28 **Abstract**

29 Crustacean aquaculture is expected to be a major source of fishery commodities in the  
30 near future. An immune priming system of shrimp is crucial for a sustainable supply, as shrimp do  
31 not have an adaptive immune system; however, little is known about their immunity. Hemocytes  
32 are known as key agents of the crustacean immune system; nevertheless, we have yet to identify  
33 the different cell types, functions, and differentiation and maturation processes associated with it.  
34 To date, only discrete and inconsistent information on the classification of shrimp hemocytes has  
35 been reported, showing that the morphological characteristics are not sufficient to resolve their  
36 actual roles. Therefore, we employed a single-cell transcriptome approach for shrimp hemocytes.  
37 Thousands of hemocytes from shrimp *Marsupenaeus japonicus* were subjected to single-cell  
38 mRNA sequencing (scRNA-seq). From the classification of cells based on their transcriptional  
39 profiles, we discovered nine different hemocyte subpopulations corresponding to different stages  
40 of the differentiation process that can be traced back to the first subpopulation. Using our  
41 classification, we also identified molecular markers for each subpopulation, and mapped their  
42 differentiation and maturation pathways. Interestingly, we also discovered growth factors that may  
43 play crucial roles during the differentiation process and provide key information for hemocyte cell  
44 culture. Among these subpopulations, different immune roles were suggested from the analysis of  
45 the differentially expressed immune-related genes. The present characterization results, based on  
46 the scRNA-seq, should set the fundamental ground for understanding shrimp immunity for the  
47 future development of shrimp aquaculture.

## 48 **Significance Statement**

49 Hemocytes are key players of the immune system in shrimps; however, their classification,  
50 maturation, and differentiation are still under debate. Our present study using single-cell RNA  
51 sequencing, revealed nine types of hemocytes based on their transcriptional profiles. We identified  
52 markers of each subpopulation and the differentiation pathways involved in their maturation. We  
53 also discovered cell growth factors that might play crucial roles in hemocyte differentiation. Different  
54 immune roles among these subpopulations were suggested from the analysis of differentially  
55 expressed immune-related genes. These results provide a unified classification of shrimp  
56 hemocytes, which improves the understanding of its immune system.

57 **Main Text**

58 **Introduction**

59 Aquaculture is an important source of animal protein and is considered one of the most  
60 important long-term growth areas of food production, providing 60% of fish for human consumption  
61 (1) (<http://www.fao.org/fishery/statistics/en>). However, crustaceans that lack an adaptive immune  
62 system (2–4) are vulnerable to pathogens. This means that ordinal vaccination is not applicable to  
63 crustaceans, unlike in fish aquaculture. Shrimp is the main target species for crustacean  
64 aquaculture. Therefore, an immune priming system for shrimp, which is entirely different from  
65 conventional vaccines, needs to be developed to control the infection of pathogens. However, little  
66 is known about the immune system of crustaceans due to the lack of biotechnological tools, such  
67 as uniform antibodies and other biomarkers (5).

68 Hemocytes, which are immune cells of crustaceans, are traditionally divided into three  
69 morphological types based on the dyeing of intracellular granules, which was established by  
70 Bauchau and colleagues (6–8). However, there have been additional reports on the classification  
71 of the hemocytes of shrimp; they were classified into four, eight, and five types based on electron  
72 microscopy (9), another dyeing method (10), and iodixanol density gradient centrifugation (11),  
73 respectively. As the morphology and dye staining properties of shrimp hemocytes are not absolute  
74 indicators, no unified understanding of their role has been established yet. Molecular markers, such  
75 as specific mRNAs, antibodies, or lectins, are usually available for characterizing the  
76 subpopulations of cells in model organisms, but this is not often the case for non-model organisms.  
77 Although monoclonal antibodies have been developed for some hemocytes of shrimp (12–18), their  
78 number is lower than that of humans, and their correspondence to the cell type, as well as their  
79 differentiation stage are under debate.

80 Recently, single-cell mRNA sequencing (scRNA-seq) techniques have dramatically  
81 changed this scene, allowing researchers to annotate non-classified cells solely based on the  
82 mRNA expression patterns of each cell. In particular, droplet-based mRNA sequencing, such as  
83 Drop-seq, developed by Macosko *et al.* (19), has gained popularity for classifying cells and  
84 identifying new cell types. The enormous amount of biological data obtained from scRNA-seq leads  
85 us to classify cells into specific groups, analyze their heterogeneity, predict the functions of single-  
86 cell populations based on the gene expression profiles, and determine the cell proliferation or  
87 development pathways based on the pseudo-time ordering of a single cell (20, 21). More recently,  
88 hemocytes of invertebrate, fly, and mosquito models have been subjected to these types of  
89 microfluidic-based scRNA-seq to reveal their functions (22, 23).

90 Here, we performed scRNA-seq analysis on *Marsupenaeus japonicus* hemocytes to  
91 classify the hemocyte types and to characterize their functions using the custom-built Drop-seq  
92 platform. To perform scRNA-seq, a high-quality gene reference is essential; however, such  
93 reference genomes are scarce for crustaceans because of the extremely high proportion of simple

94 sequence repeats (5). We circumvented this problem by preparing reference genomes using hybrid  
95 *de novo* assembly of short- and long-read RNA sequencing results. The sequences obtained from  
96 the scRNA-seq were mapped onto the reference genes successfully. Our scRNA-seq uncovered  
97 the transcriptional profiles of a few thousand *M. japonicus* hemocytes. We identified the markers of  
98 each population and the differentiation pathways associated with their maturation. We also  
99 discovered the cell growth factors that might play crucial roles in hemocyte differentiation. Different  
100 immune roles among these subpopulations were also suggested from the analysis of differentially  
101 expressed immune-related genes. Our results present a unified classification of shrimp hemocytes  
102 and a deeper understanding of the immune system of shrimp.

103

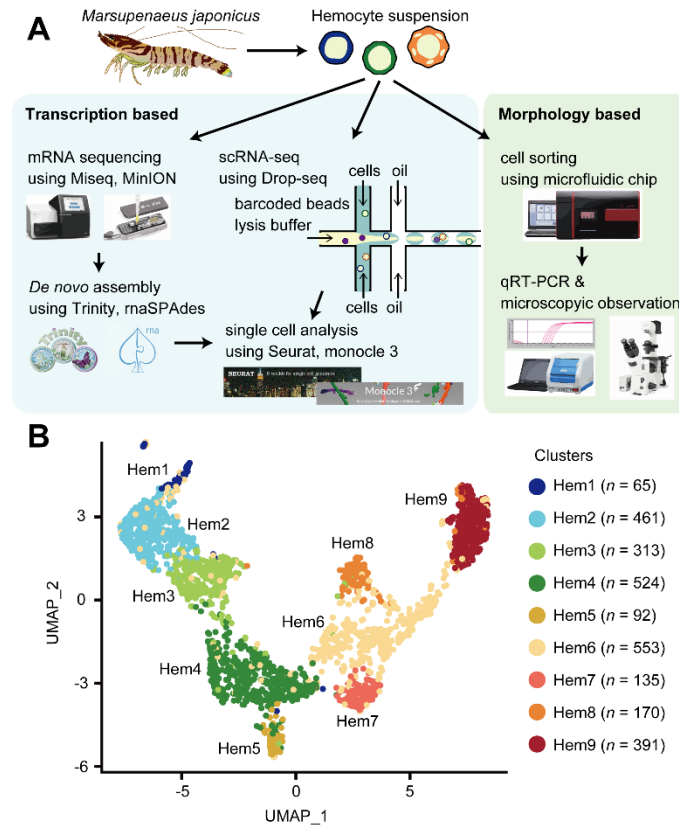
## 104 **Results**

### 105 **scRNA-seq clustering of *Marsupenaeus japonicus* hemocytes**

106 Our study utilized scRNA-seq to determine the cellular subtypes with a distinct  
107 transcriptional expression (Fig. 1 A). To map the scRNA-seq sequences from *M. japonicus*  
108 hemocytes, we first prepared *de novo* assembly of the reference genes using hybrid assembly of  
109 short- and long-read RNA sequencing results. Then, by using self-built Drop-seq microfluidic chips,  
110 single hemocytes were captured and their mRNA was barcoded using the droplet-based strategy.  
111 This process was performed in triplicates for three shrimp individuals. Following library preparation  
112 and sequencing, the transcriptomes obtained from scRNA-seq were mapped against the reference  
113 genes to discover the cell types.

114 Using the Drop-seq procedure, we profiled a total of 2,704 cells and obtained a median  
115 value of 718 unique molecular identifiers (UMIs) and 334 genes per cell across three replicates  
116 (Fig. S1 A and B). Approximately 300 genes were detected, and the total number of mRNAs  
117 expressed among individual cells varied between 100 and 1,400 (Fig. S1 C and D). There was  
118 some transcriptional variability, which may have resulted from the artifacts of the Drop-seq system,  
119 because it is consistent with the original Drop-seq paper (19) and with recent findings in other  
120 organisms, such as fish (24), flies (23), and mosquitoes (22, 25).

121 Applying the SCTransform batch correction method integrated into the Seurat package  
122 allowed us to remove the individual differences. SCTransform successfully integrated all three  
123 shrimp datasets, among which we identified a total of nine clusters (Fig. 1 B) and obtained 3,334  
124 commonly expressed genes. Each cluster contained the following number of cells: Hem 1, 65 cells  
125 (2.4%); Hem 2, 461 cells (17.0%); Hem 3, 313 cells (11.6%); Hem 4, 524 cells (19.4%); Hem 5, 92  
126 cells (3.4%); Hem 6, 553 cells (20.5%); Hem 7, 135 cells (5.0%); Hem 8, 170 cells (6.3%); and  
127 Hem 9, 391 cells (14.5%), respectively.



128  
 129 **Figure 1.** scRNA-seq of penaeid shrimp *M. japonicus* hemocytes. (A) Schematics of the  
 130 microfluidics-based scRNA-seq, preparation of the *de novo* assembled gene list, *in silico* analysis  
 131 workflow and morphology-based cell classification. (B) UMAP (uniform manifold approximation and  
 132 projection) plot of SCTransform batch corrected and integrated of hemocytes from three shrimps  
 133 ( $n = 2,704$ ).

134

### 135 Cluster specific markers and their functional prediction

136 A total of 40 cluster-specific markers were predicted using the Seurat FindMarkers tool  
 137 (Fig. 2, Dataset S1, and Dataset S2). For each cluster, seven (Hem 1), six (Hem 2), one (Hem 3),  
 138 four (Hem 4), eight (Hem 5), five (Hem 7), one (Hem 8), and eight (Hem 9) markers were selected.  
 139 Their functions were then annotated using BLASTX searching for penaeid shrimp identical proteins  
 140 downloaded from a public database.

141 Hem 1 specific markers, *histone acetyltransferase lysine acetyltransferase 6A (HAT*  
 142 *KAT6A)*, *gamma-aminobutyric acid (GABA) transporter*, and *polypyrimidine tract-binding protein 1*  
 143 *(PTBP1)* are genes related to cell proliferation, cell migration, and colony formation in human tumor  
 144 studies. HAT KAT6A is known to be a chromatin regulator that controls fundamental cellular  
 145 processes and is implicated in regulating tumor progression (26). Autocrine/paracrine signaling via  
 146 GABA receptors negatively controls ES cell and peripheral neural crest stem cell proliferation (27).

147 This GABA signaling pathway critically regulates proliferation independently of differentiation,  
148 apoptosis, and overt damage to DNA (27). PTBP1 is a multi-functional RNA-binding protein that is  
149 overexpressed in glioma, a type of tumor that occurs in the brain, and a decreased expression of  
150 PTBP inhibits cell migration and increases the adhesion of cells to fibronectin and vitronectin (28,  
151 29). PTBP has been shown to be involved in germ cell differentiation in *Drosophila melanogaster*  
152 and is essential for the development of *Xenopus laevis* (30). These pieces of evidence strongly  
153 suggest that these Hem 1 markers are related to cell proliferation in shrimp hemocytes. Among the  
154 six markers found in cluster Hem 2, three markers were annotated with hemocyte transglutaminase  
155 (HemTGase), and one marker showed high similarity with von Willebrand factor D and epidermal  
156 growth factor (EGF) domain-containing protein (VWDE). Interestingly, both Hem 1 and Hem 2  
157 showed a high expression of TGase, an immature hemocyte marker of crayfish and shrimp. When  
158 the extracellular TGase is digested, hemocytes start to differentiate into mature hemocytes (31–  
159 33). The high expression of TGase suggests that both Hem 1 and Hem 2 are in the early stage of  
160 hemocytes. In cluster Hem 3, the only identified marker showed high similarity with tubulointerstitial  
161 nephritis antigen (TINAGL). In cluster Hem 4, all markers showed similarity with the hypothetical  
162 protein.

163 In clusters Hem 5 to Hem 9, many of the cluster-specific markers showed similarity with  
164 immune-related genes of penaeid shrimp, and very few genes were unknown. We postulate that  
165 this is partly because the public database is rich in immune-related genes because of their  
166 importance. In cluster Hem 5, markers showed a high similarity with c-type lysozyme, viral  
167 responsive protein (VRP), fibrous sheath CABYR-binding (FSCB)-like, chitin binding-like protein,  
168 anti-lipop polysaccharide factor (ALF)-A1, and PDGF/VEGF-related factor 1. In cluster Hem 7,  
169 markers showed high similarity with selenium-dependent glutathione peroxidase (Se-GPX),  
170 BigPEN, ALF-C1, and hemocyte Kunitz protease inhibitor (KPI). In cluster Hem 8, the marker  
171 showed high similarity with KPI. In cluster Hem 9, the markers showed similarity with insulin-like  
172 growth factor-binding protein (IGFBP)-related protein 1, hemocyte KPI, crustacean hematopoietic  
173 factor (CHF)-like protein, single whey acidic protein domain (SWD)-containing protein, and  
174 penaeidin-II.

175 Altogether, only 70% (28/40) of markers were annotated from the BLAST searches on the  
176 penaeid shrimp identical protein data. We also performed GO annotation using eggNOG-mapper  
177 (34, 35) (<http://eggno-mapper.embl.de/>) to predict the functions of contigs, but only about 10% of  
178 the contigs were annotated, and we could not reach GO analysis.

179 From the results of this cluster-specific marker analysis, we found that Hem 1 and Hem 2  
180 are immature hemocytes. Therefore, we analyzed the whole maturation process of hemocytes  
181 using pseudo-temporal analysis. Additionally, cell growth-related genes, such as *VWDE*, *TINGAL*,  
182 *IGFBP-related protein*, and *CHF*, were identified as cluster-specific markers. We predicted their

183 functions to pursue the linkage between these genes and the hemocyte differentiation process.  
 184 Finally, the immune-related genes, which were enriched in Hem 5 to 9, were analyzed to predict  
 185 the immune function of each cluster.



186  
 187  
 188 **Figure 2.** Dot plot representing the marker genes per cluster based on the average expression  
 189 predicted using the Seurat FindMarker tool. Color gradient of the dot represents the expression  
 190 level, while the size represents the percentage of cells expressing any gene per cluster.

191  
 192 **Pseudo temporal ordering of cells delineates hemocyte lineages**

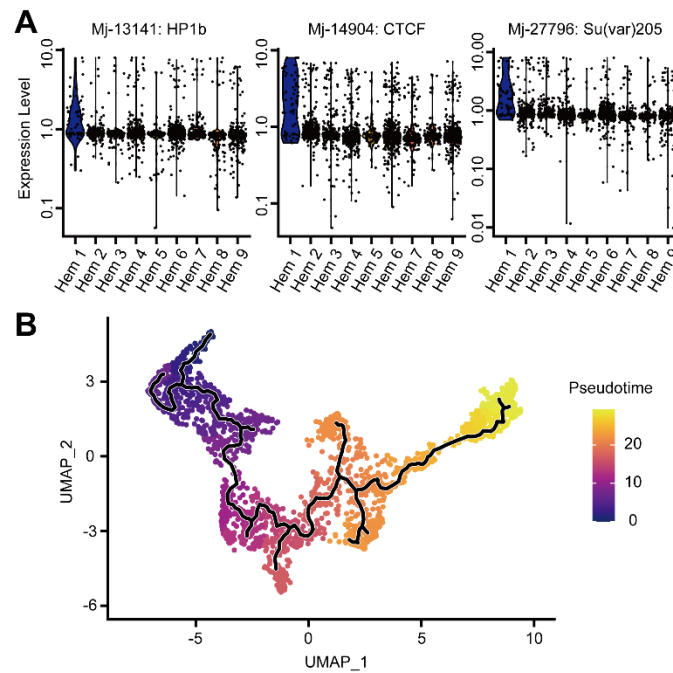
193 To investigate the dynamics of hemocyte differentiation, we performed lineage-tree  
 194 reconstruction using the monocle3 learn\_graph function. The differentiation and proliferation of  
 195 hemocytes in shrimp and other crustaceans are still under debate (36). Since the cell cycle- and  
 196 hemocyte-type-specific markers are better studied in *Drosophila*, we checked the commonly  
 197 expressed genes of *M. japonicus* that are similar to the markers of *Drosophila* to determine whether  
 198 they are present in shrimp. In the search for cell cycle-specific markers (Dataset S3), a large portion

199 of cells in Hem 1 expressed the G2/M-related genes of *Drosophila: heterochromatin protein 1b*  
200 (*HP1b*); Mj-13141, *CCCTC-binding factor (CTCF)*; Mj-14904, *suppressor of variegation 205*  
201 (*Su(var)205*); Mj-27796 (Fig. 3 A and Fig. S2). *Drosophila HP1* and *Su(var)205* are known to be  
202 essential for the maintenance of the active transcription of the euchromatic genes functionally  
203 involved in cell-cycle progression, including those required for DNA replication and mitosis (37, 38).  
204 CTCF has zinc finger domains and plays an important role in the development and cell division of  
205 fly and mammalian cells (39, 40). In the BLAST search of two genes related to cell-cycle  
206 progression, that is, Mj-13141 and Mj-27796, on identical proteins of penaeid shrimp, they showed  
207 high similarity with the *chromobox protein homolog 1-like* (Dataset S1). A chromobox family protein  
208 contributes to lymphomagenesis by enhancing stem cell self-renewal and/or by increasing the  
209 replicative potential of cancer stem cells in human tumor cells (41). BLAST search of Mj-14904 on  
210 identical proteins of penaeid shrimp showed similarity with the zinc finger protein that contains the  
211 same domain of CTCF (Dataset S1). These findings suggested that hemocytes grouped as Hem 1  
212 are tightly regulated by these G2/M phase-related genes to promote cell division.

213 Among the specific markers of four types of *Drosophila* hemocytes, four genes in  
214 prohemocytes, 11 genes in plasmatocytes, 11 genes in lamellocytes, and 6 genes in crystal cells  
215 showed similarity with the shrimp genes (Dataset S4). However, no genes were significantly  
216 expressed in certain clusters (Fig. S3). Therefore, we concluded that these *Drosophila* hemocyte  
217 markers cannot be adapted as markers for the hemocytes of shrimp.

218 We considered Hem 1 to be the initial state of hemocytes and set it as the starting point in  
219 the differentiation process because Hem 1 expressed cell proliferation-related genes, TGase (an  
220 immature hemocyte marker), and G2/M phase-related genes (37–42). From this pseudo temporal  
221 ordering analysis, we found four main lineages starting from Hem 1 to Hem 5, Hem 7, Hem 8, and  
222 Hem 9 at the endpoints (Fig. 3 B and Fig. S4 A-D). In crayfish, hematopoietic stem cells are present  
223 in hematopoietic tissue (HPT), and two types of hemocyte lineages starting from a hematopoietic  
224 stem cell exist (43). In *Penaeus monodon*, hyaline cells (i.e., agranulocytes) are considered as the  
225 young and immature hemocytes of two types of matured hemocytes (9). Our pseudo temporal  
226 ordering analysis revealed that the hemocytes of *M. japonicus* differentiate from a single  
227 subpopulation into four major populations. The differentiation process of *M. japonicus* hemocytes  
228 was continuous, not discrete, which was in agreement with previous arguments on the crustacean  
229 hematopoiesis mechanism (9, 43, 44).





230  
231 **Figure 3.** Pseudo temporal ordering of hemocyte lineages. (A) Violin plots displaying normalized  
232 expression levels of each cell cycle related genes across all clusters. (B) Visualization of clusters  
233 (from Figure 1B) onto the pseudo time map using monocle 3.

234

### 235 **Expression of cell growth-related genes**

236 The exploration of cluster-specific markers revealed that cell growth-related genes were  
237 specifically expressed in certain clusters. Therefore, we highlighted five genes that are predicted  
238 to be involved in cell growth and differentiation: *VWDE-like*, *TINAGL*, *PDGF/VEGF-related factor*  
239 *1*, *IGFBP-related protein 1*, and *CHF-like* (Fig. 4, Fig. S5, and Dataset S5).

240 *VWDE-like* was highly expressed in clusters Hem 1 to Hem 3 (Fig. 4 A and B). The  
241 expression of *VWDE* is a common feature of blastemas, which are capable of regenerating limbs  
242 and fins in a variety of highly regenerative species (45). *VWDE* contains several epidermal growth  
243 factor (EGF) domains and is expected to be a downstream effector once a blastema has been  
244 established, but it is not a driver of blastema formation (45). *VWDE-like* of *M. japonicus* was  
245 expressed more strongly in Hem 2 than in Hem 1, indicating that *VWDE-like* also works as a  
246 downstream effector against Hem 1, which is predicted to be composed of undifferentiated  
247 hemocytes.

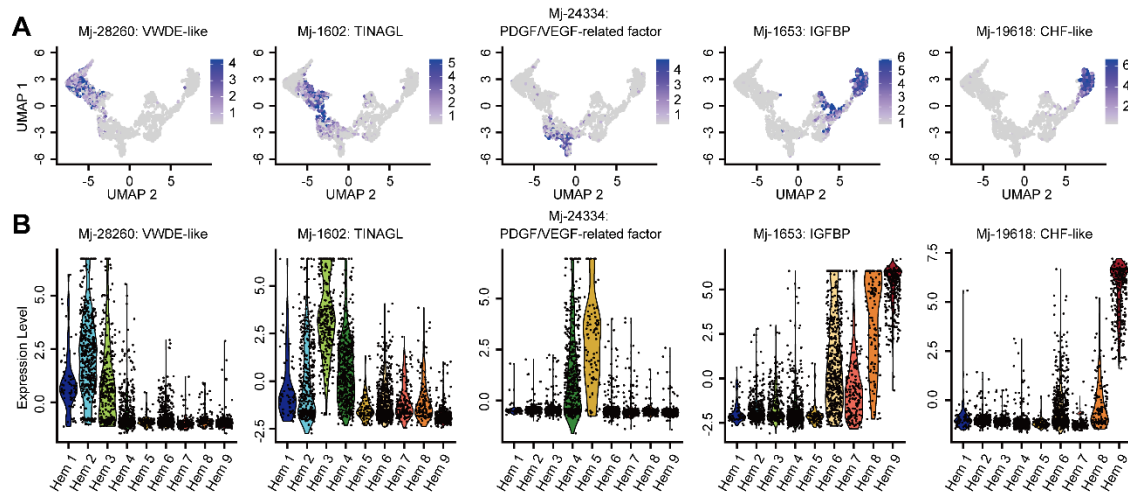
248 *TINAGL*, which was expressed in Hem 3 and 4, is a secreted extracellular protein that is  
249 essential for early angiogenesis in developing zebrafish embryos (46) and humans (47). *TINAGL*  
250 of *M. japonicus* has been proposed to participate in angiogenic cell differentiation. *TINAGL* is also  
251 known as a suppressor of cancer progression and metastasis by binding to receptors of EGF in

252 humans (48). Interestingly, TINAGL of *M. japonicus* was expressed in Hem 3 and Hem 4, in which  
253 the expression of VWDE-like was weakened (Fig. 4 A and B). This suggests that TINAGL might  
254 suppress the differentiation function of VWDE-like in Hem 3 and 4 in shrimp.

255 Cells expressing PDGF/VEGF-related factors were dominant in Hem 4 and Hem 5 (Fig. 4  
256 A and B). The vascular endothelial growth factor (VEGF) signaling pathway is essential for  
257 vasculogenesis, cell proliferation, and tumor migration in mammals (49, 50). Furthermore, in  
258 *Drosophila*, VEGF homologs control the number of circulating hemocytes (51). The high expression  
259 of PDGF/VEGF-related factors in Hem 4 and Hem 5 showed that Hem 3 would differentiate into  
260 Hem 5 through Hem 4 via the VEGF signaling pathway.

261 Hem 6 to Hem 9 expressed insulin-like growth factor (IGF) binding protein (IGFBP) (Fig. 4  
262 A and B). IGFBP delivers IGFs to the target cells in mammal studies and is essential for cell growth  
263 or differentiation (52). The high expression of a receptor of the insulin-like peptide at mature  
264 hemocytes in the mosquito suggests that the insulin signaling pathway regulates hemocyte  
265 proliferation (53). The silencing and overexpression of IGFBP caused a decrease and increase in  
266 the growth of hemocytes, respectively, in the loss and gain function study of abalone *Haliotis*  
267 *diversicolor* (54). These studies indicate that the IGFBP-related insulin signaling pathway is  
268 important for hemocyte proliferation and differentiation in invertebrates. IGFBP might play an  
269 essential role in the differentiation of hemocytes from Hem 4 to Hem 6–9 in shrimp. The high  
270 expression of IGFBP is determined in the brain and gonads of *Litopenaeus vannamei* (55). This  
271 fact also suggests that IGFBP plays a possible role in organ growth and maturation in shrimp.

272 Up to this point, the analyzed genes were proliferation- and differentiation-promoting, but  
273 there was also the specific expression of the hemocyte homeostasis regulatory gene, crustacean  
274 hematopoietic factor (CHF) (43) (Fig. 4 A and B). CHF is a hematopoietic factor of crayfish, and  
275 the silencing of CHF leads to an increase in the apoptosis of cells in HPT, and a reduction in the  
276 number of circulating hemocytes (33). Additionally, the silencing of laminin, a receptor of CHF,  
277 reduces the number of circulating hemocytes by decreasing the number of agranulocytes, as  
278 opposed to granulocytes, in *P. vannamei* (55). CHF-like was expressed at cluster Hem 9 (Fig. 4 A  
279 and B), in which hemocytes are predicted to be matched here. Taken together, CHF-like expressed  
280 from matured hemocytes, Hem 9, might work as a hematopoietic factor against agranulocytes or  
281 regulate the homeostasis of agranulocytes.



282  
283 **Figure 4.** Cell growth-related gene expression across all clusters. (A) Expression pattern of the cell  
284 growth-related genes across cell clusters. (B) Violin plots displaying normalized expression levels  
285 of each cell growth-related genes across all clusters.

286

### 287 Expression of immune-related genes in single cells

288 Hemocytes of shrimp play key roles in their immunity; therefore, we selected immune-  
289 related genes from 3,334 commonly expressed genes, and then analyzed their expression levels  
290 to deduce the detailed immune functions of each cluster.

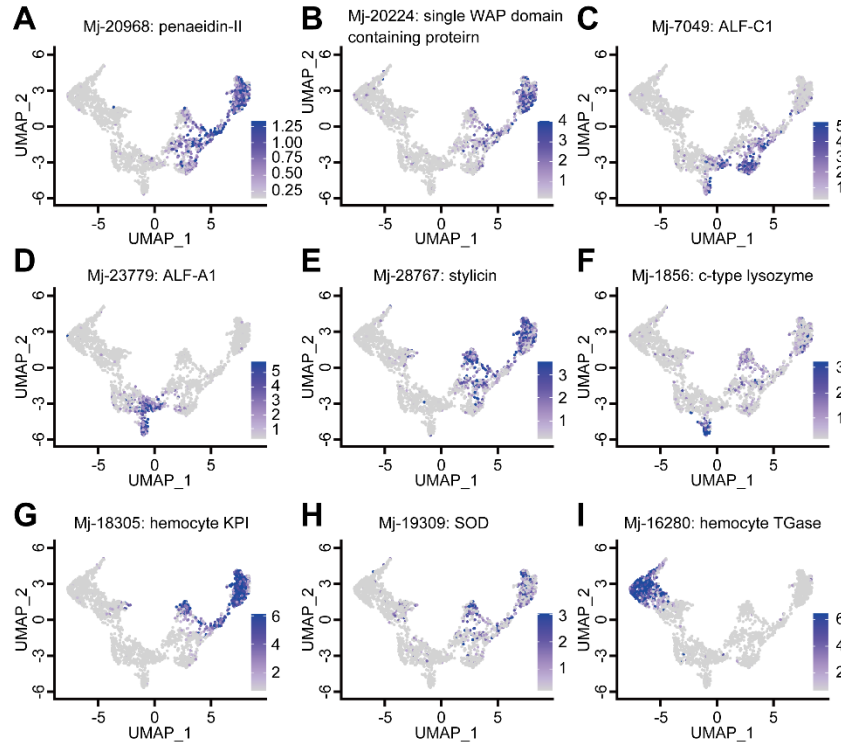
291 Antimicrobial peptides (AMPs) play the most important role in the immunity of shrimps and  
292 are well known to be stored in granulocytes (56, 57). The expression patterns of AMPs revealed  
293 that the major AMPs of penaeid shrimp were expressed in clusters Hem 5 to Hem 9 (Fig. 5 A-F,  
294 Fig. S6 and Dataset S6). Therefore, Hem 5 to Hem 9 were predicted to be granulocytes. These  
295 AMP-expressing clusters were broadly classified into two groups. One group was Hem 5, which  
296 expressed several AMPs, such as ALF-A1 and c-type lysozyme (Fig. 5 D and F), but also  
297 expressed other immune-related genes different from AMPs: *chitin-binding protein* and *virus*  
298 *responsible protein* (VRP) (Fig. 2). Chitin-binding protein is located on the cell surface and interacts  
299 with virus envelope proteins in shrimp (58). VRP is distributed in granulocytes, and infection by  
300 pathogenic viruses causes an increase in VRP transcripts (59). The other group is Hem 6 to 9,  
301 which strongly expresses major AMPs, such as penaeidin, stylicin, and SWD, suggesting that this  
302 group corresponds to the most studied immune-related cell subpopulation to date. The level of  
303 penaeidin-positive hemocytes is increased after bacterial infection (60), but is reduced after a virus  
304 infection (61). Stylicin and SWD mRNA expression was decreased after virus infection in *M.*  
305 *japonicus* and *P. monodon*.

306 Together, the functions of these two groups can be characterized as follows. In Hem 5,  
307 VRP, whose level is known to be increased by viral infection, was specifically expressed, while

308 AMPs were downregulated. Thus, Hem 5 is predicted to be the group that contributes to the  
309 immune response against viruses. Additionally, a virus infection causes an increase in the  
310 expression of both VEGF and its receptors in hemocytes to regulate a downstream signaling  
311 pathway (62–64). The high expression of PDGF/VEGF-related factors at Hem 5 (Fig. 2 and 4)  
312 supports our prediction that Hem 5 plays an essential role in shrimp biodefense against viruses.  
313 Previously, a subtype of granulocytes, termed semi-granular cells (SGC), were isolated from *L.*  
314 *vannamei*, in which lysozyme was highly expressed. It is possible that Hem 5 in *M. japonicus*  
315 corresponds to SGC found in *L. vannamei* because c-type lysozyme was strongly expressed in  
316 Hem 5, in our study. Conversely, the AMPs specifically expressed at Hem 6–9 were upregulated  
317 by bacterial infection. Therefore, these clusters contribute to bacterial defense. Different types of  
318 ALF play different roles in shrimp immunity, which improves the synergism in shrimp antimicrobial  
319 defenses (65). The expression patterns of ALFs were also different in each cluster (Fig. 5 C and D,  
320 Fig. S6 and Dataset S6), suggesting that different clusters have different immunological functions.

321 Some of the hemocyte-type-specific markers related to their immune function have been  
322 studied in crayfish: prophenoloxidase (proPO) in matured hemocytes, copper/zinc superoxide  
323 dismutase (SOD) in SGC, and Kazal-type proteinase inhibitor (KPI) in granular cells (GC), and  
324 transglutaminase (TGase) in immature cells (66). We BLAST searched homologies between these  
325 genes and common expressed genes to check their potential as specific markers. As a result, 31  
326 genes were found to have homology with the genes listed above (Fig. S6 and Dataset S6). TGase  
327 was strongly expressed in immature clusters Hem 1 and Hem 2, and can, therefore, be used as a  
328 marker of immature hemocytes (Fig. 5 I and Fig. S6). ProPOs were not highly expressed in the  
329 present single-cell study. Both KPI and SOD were mostly expressed at both Hem 8 and Hem 9,  
330 and their expression levels were similar between these clusters (Fig. 5 G and H and Fig. S6). These  
331 results suggest that the functional segregation of hemocytes in shrimp is different from that in  
332 crayfish, in which these molecular markers are expressed distinctly between GC and SGC. The  
333 KPI of *M. japonicus* is expressed in only some hemocytes in healthy shrimps, and bacterial infection  
334 causes an increase in KPI expression (67). Therefore, it can be predicted that the number of KPI-  
335 positive hemocytes in Hem 8 and 9 would be increased upon a pathogen infection, in shrimp.

336 In the mosquito, scRNA-seq revealed a new subpopulation called “antimicrobial  
337 granulocytes” that expressed characteristic AMPs (22). Similarly, in *M. japonicus*, the expression  
338 patterns of immune-related genes were also different among certain clusters, suggesting that  
339 shrimp hemocytes are more heterogeneous than previously thought. It is anticipated that the class  
340 of granulocytes discussed in previous studies is actually a mixture of clusters exhibiting different  
341 roles.



342

343

**Figure 5.** Expression pattern of the immune-related genes across cell clusters. (A) Penaeidin-II, (B) single WAP domain containing protein, (C) ALF-CA, (D) ALF-A1, (E) stylicin, (F) c-type lysozyme, (G) KPI, (H) SOD, and (I) TGase.

346

### 347 Validation of marker genes and the relationship between clusters and morphology

348

Our scRNA-seq results revealed nine major subpopulations and their marker genes, and the possible differentiation trajectory of *M. japonicus* hemocytes. Next, we examined the correlation between the morphology and expression of marker genes. Two major populations of hemocytes were sorted based on the forward versus side scatter plot obtained using microfluidic-based fluorescence-activated cell sorter (FACS). The sorted populations were observed using microscopy. FACS was able to separate hemocytes into two morphologically different populations (Fig. 6 A–E): smaller cells with low internal complexity in region 1 (R1) ( $50.7\% \pm 5.2\%$ ) and larger cells with high internal complexity in region 2 (R2) ( $47.7\% \pm 3.4\%$ ). From DIC and dye staining imaging (Fig. 6 A and B), we observed that cells in the R1 region contained no or few granules in the cytoplasm. The nucleus occupied a large portion of the volume in these cells (Fig. 6 C). Conversely, those in the R2 region had many granules in the cytoplasmic region, which occupied a large portion of cells (Fig. 6 D).

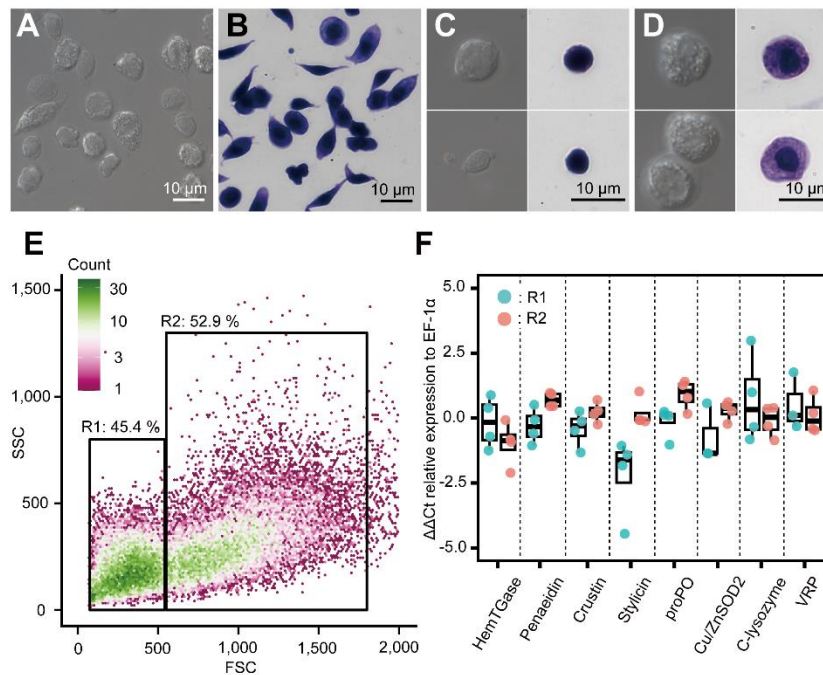
360

361

362

We conducted qRT-PCR analysis to determine the expression of some representative genes in these populations. The results showed that the  $\Delta\Delta Ct$  values of the transcripts of HemTGase were higher in R1 hemocytes than in R2 hemocytes, while the values of penaeidin,

363 crustin, stlyicin, proPO, and Cu/ZnSOD2 were higher in R2 hemocytes (Fig. 6 F). The  $\Delta\Delta Ct$  values  
364 of transcripts of c-type lysozyme and VRP were similar in R1 and R2 hemocytes. The combination  
365 of FACS and qRT-PCR results confirmed that the gene expression of the two populations in shrimp  
366 hemocytes was roughly divided based on morphology, that is, agranulocytes and granulocytes,  
367 which is consistent with our scRNA-seq analysis. Granulocytes found in the R2 region expressed  
368 major AMPs, such as penaeidin, crustin, and stlyicin, suggesting that they consist of clusters Hem  
369 6 to Hem 9. However, c-type lysozyme and VRP, which are markers of Hem 5 (Fig. 2), were  
370 expressed in cells in both R1 and R2 regions, indicating that Hem 5 exists in both populations and  
371 is indistinguishable from the morphological characteristics. The number of cells occupying R1 and  
372 R2 was  $50.7\% \pm 5.2\%$  and  $47.7\% \pm 3.4\%$  (from  $n = 4$ ), while the total number of cells classified as  
373 Hem 1 – 4 and Hem 5 – 9 in our single-cell analysis was  $50.4\%$  (1,363 cells) and  $49.6\%$  (1,341  
374 cells), respectively.



375 **Figure 6.** Morphological analysis of hemocytes and transcript profiles based on morphology. (A)  
376 DIC (Differential Interference Contrast) image of unsorted total hemocytes. (B) Dye stained total  
378 hemocytes. (C) DIC imaging and dye staining of R1 sorted hemocytes. (D) DIC imaging and dye  
379 staining of R2 sorted hemocytes. (E) FACS (fluorescence-activated cell sorting) analysis of  
380 hemocytes. Based on the FSC (forward scatter) and SSC (side scatter) two-dimensional space,  
381 two regions (R1 and R2) were obtained. (F) Differential gene expression analysis between R1 and  
382 R2 of hemocytes sorted using FACS.  $\Delta\Delta Ct$  values were analyzed using qRT-PCR. Higher  $\Delta\Delta Ct$   
383 values indicate a higher accumulation of mRNA transcripts.

## 384 Discussion

385 Our single-cell transcriptome analysis revealed that there are nine subpopulations of  
386 hemocytes in shrimp. This result differs from any previous classification strategy based on various  
387 approaches, such as simple staining (7–9), monoclonal antibodies (18), flow cytometry (68), and  
388 lectin-binding profiles (69). We hope that future studies will clarify the relationships between these  
389 phenotypic features and our classification to comprehend the role of each cluster in the immune  
390 system of shrimp.

391 The cluster-specific markers and cell proliferation-related genes found here helped us to  
392 understand how shrimp hemocytes differentiate. A strong expression of TGase, cell proliferation,  
393 and G2/M state-related genes in Hem 1 suggested that hemocytes in this cluster are oligopotent  
394 and located upstream in the differentiation process. In crustaceans, especially shrimp and crayfish,  
395 it is known that hemocytes are produced in HPT, and that differentiated hematopoietic cells from  
396 HPT circulate in the body fluid (9, 36, 66). However, G2/M state hemocytes of *M. japonicus* exist  
397 in the hemolymph and account for only  $0.63\% \pm 0.28\%$  of the circulating hemocytes (70). Hem 1  
398 accounts for only 2.4% of the analyzed cells. This similarity in the fraction also indicates that only  
399 a very small fraction of oligopotent or initial state hemocytes exist among the circulating  
400 hemocytes.

401 Our results also revealed that the growth-related genes were expressed at specific clusters  
402 (Fig. 4 A and B). From these results, we propose that shrimp hemocytes differentiate as follows  
403 (Fig. 7 A and B): 1) Hem 1 is the initial state of circulating hemocytes and has an oligopotent ability,  
404 which leaked out from HPT; 2) Hem 3 is differentiated from Hem 1 by VWDE-like through Hem 2;  
405 3) Hem 4 is differentiated from Hem 3 by TINAGL; 4) Hem 5 is differentiated from Hem 4 by  
406 PDGF/VEGF-related factor; 5) Hem 7 to Hem 9 are differentiated from Hem 4 by IGFBP-related  
407 protein through Hem 6; 6) CHF-like is expressed in Hem 9 to maintain the immature hemocytes,  
408 Hem 1 to Hem 4. Loss and gain function studies of these differentiating factors are necessary to  
409 prove the full differentiation process of penaeid shrimp hemocytes. Since we identified a group of  
410 proliferating cells and differentiation factors here, the next step is to establish a way to isolate and  
411 cultivate them. The markers of each cluster identified here will be good tools for isolating specific  
412 cell types.

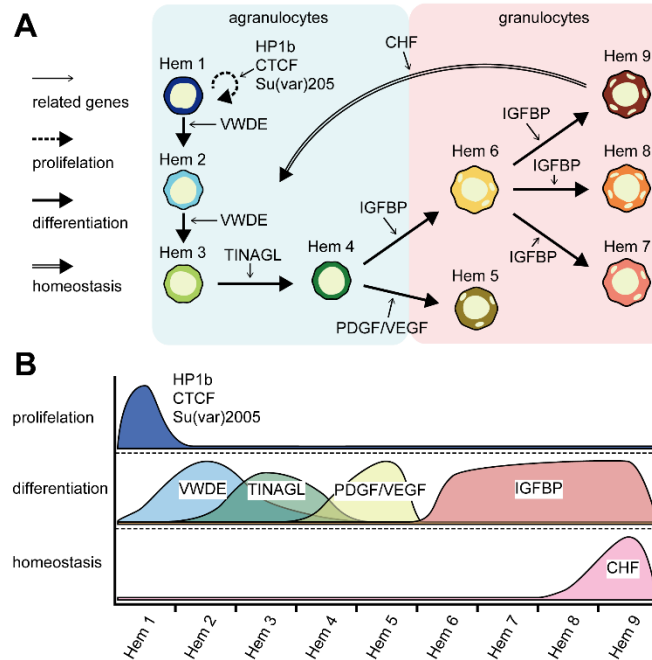
413 Crayfish's hemocytes and *Drosophila* hemocytes have been classified into three and four  
414 major types according to the marker genes, respectively (23, 36). However, these crayfish or  
415 *Drosophila* marker genes were found to be inadequate as cluster-specific markers for penaeid  
416 shrimp in our study. Insects and crustaceans are thought to become independent about 500 million  
417 years ago (71, 72), and shrimp and crayfish are thought to have become evolutionarily independent  
418 about 450 million years ago (73). Thus, it is straightforward to reason that the functions of these  
419 genes have changed during the evolutionary process. Therefore, we should not simply argue that

420 the morphological and functional similarities between shrimp and *Drosophila*/crayfish hemocytes  
421 are the same.

422 Most of the markers that were characteristically expressed in Hem 1 and Hem 4 could not  
423 be functionally predicted by the BLAST search (Fig. 2). We speculate that the characteristic genes  
424 of Hem 1 are associated with cell duplication and that Hem 4 is associated with the regulation of  
425 cell differentiation. The division and differentiation mechanisms of shrimp hemocytes are still largely  
426 unknown, and no techniques on culture shrimp hemocytes *in vitro* have been reported. The analysis  
427 of these unknown gene characteristics may reveal these mechanisms. Notably, no specific marker  
428 gene was found in Hem 6, probably because these cells are yet to be specialized, unlike those in  
429 Hem 7 to Hem 9.

430 In conclusion, we succeeded in classifying shrimp hemocytes into nine subpopulations  
431 based on their transcriptional profiles, while they were only classified into two groups using FACS.  
432 Furthermore, our results imply that hemocytes differentiate from a single initial population. Although  
433 we have not yet successfully cultured crustacean hemocytes in passaging cultures, information on  
434 these subpopulations and marker genes will provide a foothold for hemocyte culture studies.  
435 Despite our success in the classification of hemocytes, we have not yet been able to fully  
436 understand the functions of each hemocyte group in detail. One reason for this is that the functions  
437 of some marker genes are still unknown. The present single-cell transcriptome data serves as a  
438 platform providing the necessary information for the continuous study of shrimp genes and their  
439 functions. Additionally, we have only determined the subpopulations of hemocytes in the normal  
440 state, so that our next goal will be to analyze the hemocytes in the infected state of certain diseases  
441 at different levels of cell maturation. In this way, we will be able to identify the major subpopulations  
442 that may work against the infectious agent. Likewise, it will be interesting to see how hemocytes  
443 from fertilized eggs mature. Additionally, single-cell analysis of hematopoietic tissues can also be  
444 expected to reveal more detailed differentiation mechanisms. Unlike terrestrial invertebrates, such  
445 as *Drosophila* and mosquitoes, shrimps are creatures that live in the ocean and are evolutionarily  
446 distant from each other. Understanding the immune system of shrimp species will require  
447 continuous effort, but we believe that it will provide efficient solutions to aquaculture problems.





448

449

**Figure 7.** Model of the roles of cell growth-related genes in hemocyte differentiation. (A) Shrimp hemocyte differentiation process, 1) Hem 1 is the initial state of circulating hemocytes, which have oligopotent ability, which leaked out from the hematopoietic tissue (HPT); 2) Hem 3 is differentiated from Hem 1 by VWDE-like through Hem 2; 3) Hem 4 is differentiated from Hem 3 by TINAGL; 4) Hem 5 is differentiated from Hem 4 by PDGF/VEGF-related factor; 5) Hem 7 to Hem 9 are differentiated from Hem 4 by IGFBP-related protein through Hem 6; 6) CHF-like is expressed in Hem 9 to maintain the immature hemocytes, Hem 1 to Hem 4. (B) Schematics of cell growth or homeostasis-related gene expression across clusters. The gene expression distribution was cluster-specific.

456

457

458

459

## Materials and Methods

460

### Shrimp and cell preparation

461

Twenty-three female kuruma shrimp, *Marsupenaeus japonicus*, with an average weight of 20 g, were purchased from a local distributor and maintained in artificial seawater with a 34 ppt salinity with a recirculating system at 20°C. Hemolymph was collected using an anticoagulant solution suitable for penaeid shrimp (7) from an abdominal site. The collected hemolymph was centrifuged at 800 x g for 10 min to collect the hemocytes, which were then washed twice with PBS

465

466 and the osmolarity was adjusted to kuruma shrimp (KPBS: 480 mM NaCl, 2.7 mM KCl, 8.1 mM  
467 Na<sub>2</sub>HPO<sub>4</sub>·12H<sub>2</sub>O, 1.47 mM KH<sub>2</sub>PO<sub>4</sub>, pH 7.4).

468

#### 469 **Preparation of expressing gene list of hemocytes**

470 *De novo* assembled transcript data were prepared as a reference for mapping Drop-seq  
471 data, because the genome sequence of *M. japonicus* is still unknown. To improve the quality of the  
472 *de novo* assembled transcript sequences, we prepared long-read mRNA sequences using MinION  
473 (Oxford Nanopore Technologies) direct RNA sequencing to conduct hybrid *de novo* assembly.  
474 Poly(A) tailed RNA was purified from 58 µg of total RNA from the hemocytes of 16 shrimp using  
475 Dynabeads Oligo(dT)<sub>25</sub> (Thermo Fisher Scientific), and 500 ng of poly-(A) RNA was ligated to  
476 adaptors using a direct RNA sequencing kit (Oxford Nanopore Technologies) according to the  
477 manufacturer's manual version DRS\_9080\_v2\_revL\_14Aug2019. Finally, 44 ng of the library was  
478 obtained and sequenced using MinION, by using a MinION flow cell R9.4.1 (Oxford Nanopore  
479 Technologies). All sequencing experiments were performed using MinKNOW v3.6.5 without base  
480 calling. Raw sequence data were then base-called using Guppy v3.6.1. Once the raw signal from  
481 the MinION fast5 files was converted into fastq files, the sequencing errors were corrected using  
482 TALC v1.01 (74)(<https://gitlab.igh.cnrs.fr/lbroseus/TALC>) by using the Illumina short reads  
483 sequence of kuruma shrimp hemocytes (DDBJ Sequence Read Archive (DRA) accession number  
484 DRA004781). The corrected long-read sequences from MinION and short-read sequences from  
485 Illumina Miseq were hybrid *de novo* assembled using rnaSPAdes v3.14.1  
486 (75)(<https://cab.spbu.ru/software/rnaspades/>) and Trinity 2.10.0  
487 (76)(<https://github.com/trinityrnaseq/trinityrnaseq/wiki>). All assembled *de novo* transcripts were  
488 merged and subjected to the EvidentialGene program v2022.01.20  
489 (<http://arthropods.eugenec.org/EvidentialGene/>) to remove similar sequences with a default  
490 parameter. The remaining sequences were renamed as Mj-XXX and used as a hemocyte-  
491 expressing gene list. The assembled sequences and code used to perform base-calling and *de*  
492 *nov*o assembly are available on GitHub at [https://github.com/KeiichiroKOIWA/Drop-](https://github.com/KeiichiroKOIWA/Drop-seq_on_shrimp)  
493 [seq on shrimp](https://github.com/KeiichiroKOIWA/Drop-seq_on_shrimp).

494

#### 495 **Single-cell and single-bead encapsulation by a microfluidic device and exonuclease and** 496 **reverse transcribe reaction on a bead**

497 The drop-seq procedure was used to encapsulate single hemocytes and single mRNA  
498 capture beads together into fL-scale microdroplets, as previously described (19). The following  
499 steps were performed in triplicates for three shrimp individuals. Briefly, the self-built Drop-seq  
500 microfluidic device was prepared by molding polydimethylsiloxane (PDMS; Sylgard 184, Dow  
501 Corning Corp.) from the microchannel structure formed by the negative photoresist (SU-8 3050,

502 Nippon Kayaku Co.). Using this device, droplets containing a cell and a Barcoded Bead SeqB  
503 (ChemGenes Corporation) were produced up to 2 mL per sample using a pressure pump system  
504 (Droplet generator, On-chip Biotechnologies Co., Ltd.). During the sample introduction, the vial  
505 bottles containing cells and beads were shaken using a vortex mixer to prevent sedimentation and  
506 aggregation (77). Droplets were collected from the channel outlet into the 50-mL corning tube and  
507 incubated at 80°C for 10 min in a water bath to promote hybridization of the poly(A) tail of mRNA  
508 and oligo d(T) on beads. After incubation, droplets were broken promptly and barcoded beads with  
509 captured transcriptomes were reverse transcribed using Maxima H Minus Reverse Transcriptase  
510 (Thermo Fisher Scientific) at RT for 30 min, then at 42°C for 90 min. Then, the beads were treated  
511 with Exonuclease I (New England Biolabs) to obtain single-cell transcriptomes attached to  
512 microparticles (STAMP). The first-strand cDNAs on beads were amplified using PCR. The beads  
513 obtained above were distributed throughout PCR tubes (1,000 beads per tube), wherein 1× KAPA  
514 HiFi HS Ready Mix (KAPA Biosystems) and 0.8 μM 1<sup>st</sup> PCR primer were included in a 25 μL  
515 reaction volume. PCR amplification was achieved using the following program: initial denaturation  
516 at 95°C for 3 min; 4 cycles at 98°C for 20 s, 65°C for 45 s, and 72°C for 6 min; 12 cycles of 98°C  
517 for 20 s, 67°C for 20 s, and 72°C for 6 min; and a final extension at 72°C for 5 min. The amplicons  
518 were pooled, double-purified with 0.9× AMPure XP beads (Beckman Coulter), and eluted in 100 μL  
519 of ddH<sub>2</sub>O. Sequence-ready libraries were prepared according to Picelli *et al.* (78). A total of 1 ng of  
520 each cDNA library was fragmented using home-made Tn5 transposome in a solution containing 10  
521 mM TAPS-NaOH (pH 8.5), 5 mM MgCl<sub>2</sub>, and 10% dimethylformamide at 55°C for 10 min. The  
522 cDNA fragments were purified using a DNA Clean & Concentrator Kit (Zymo Research) and eluted  
523 in 25 μL of ddH<sub>2</sub>O. The index PCR reaction was performed by adding 12 μL of the elute to a mixture  
524 consisting of 1× Fidelity Buffer, 0.3 mM dNTPs, 0.5 U KAPA HiFi DNA polymerase (KAPA  
525 Biosystems), 0.2 μM P5 universal primer, and 0.2 μM i7 index primer. Each reaction was achieved  
526 as follows: initial extension and subsequent denaturation at 72°C for 3 min and 98°C for 30 s; 12  
527 cycles of 98°C for 10 s, 63°C for 30 s, and 72°C for 30 s; and a final extension at 72°C for 5 min.  
528 The amplified library was purified using 0.9× AMPure XP beads and sequenced (paired-end) on an  
529 Illumina NextSeq 500 sequencer (NextSeq 500/550 High Output v2 kit (75 cycles); 20 cycles for  
530 read1 with custom sequence primer, 8 cycles for index read, 64 cycles for read2. Before performing  
531 the Drop-seq on kuruma shrimp hemocytes, we validated the protocol by performing the same  
532 procedure using a mixture of HEK293 and NIH3T3 cells and sequencing the test library using a  
533 Miseq Reagent Kit v3 (150 cycles).

534

### 535 **Analysis of single-cell data**

536 Paired-end reads were processed and mapped to the reference *de novo* assembled gene  
537 list of hemocytes following the Drop-seq Core Computational Protocol version 2.0.0, and the

538 corresponding Drop-seq tools v2.3.0 (<https://github.com/broadinstitute/Drop-seq>) provided by  
539 McCarroll Lab (<http://mccarrollab.org/dropseq/>). The Picard suite  
540 (<https://github.com/broadinstitute/picard>) was used to generate the unaligned bam files. The steps  
541 included the detection of barcode and UMI sequences, filtration and trimming of low-quality bases  
542 and adaptors or poly(A) tails, and the alignment of reads using bowtie2 v2.4.1 (79) ([http://bowtie-  
543 bio.sourceforge.net/bowtie2/index.shtml](http://bowtie-bio.sourceforge.net/bowtie2/index.shtml)). The cumulative distribution of reads from the aligned  
544 bam files was obtained using BAMTagHistogram, and the number of cells was inferred using Drop-  
545 seq tools.

546

#### 547 **Data integration**

548 After digital expression data from 3 shrimps were read using Seurat v3.2.1 (80,  
549 81)(<https://satijalab.org/seurat/>), SCTransform (81) was performed to remove the technical  
550 variation and to select common expressing genes, while retaining biological heterogeneity. We ran  
551 a PCA using the expression matrix of the top 3,000 most variable genes. The total number of  
552 principal components (PCs) required to compute and store was 50. The UMAP was then performed  
553 using the following parameters: n.neighbors, min.dist, and n.components were 10L, 0.1, and 2,  
554 respectively, to visualize the data in the two-dimensional space, and then the clusters were  
555 predicted with a resolution of 0.5.

556

#### 557 **Functional prediction of commonly expressed genes**

558 The predicted functions of selected assembled sequences as common expressing genes  
559 across three replicates were searched using BLAST program v2.2.31 (82, 83)  
560 (<https://ftp.ncbi.nlm.nih.gov/blast/executables/blast+/LATEST/>) on penaeid shrimp identical  
561 proteins (downloaded from NCBI Identical Protein Groups on 19th of August, 2020) with the blastx  
562 parameter of e-value as 0.0001 and num\_alignments as 3. Then, the functions of each cluster were  
563 predicted based on the marker genes. Marker genes were predicted using the Seurat  
564 FindAllMarkers tool with the following parameters: min.pct as 0.5, logfc.threshold as 1, and test.

565

#### 566 **Visualization of genes with distinctive functions on single hemocytes**

567 To visualize the genes with distinctive functions of shrimp, we extracted the distinct  
568 sequences from commonly expressed genes based on their blastx results against penaeid shrimp  
569 identical proteins. Here, we focused on the cell growth-related genes listed in Dataset S5 and on  
570 immune-related genes, such as antimicrobial peptides (AMPs), transglutaminase, copper/zinc  
571 superoxide dismutase, and Kazal-type proteinase inhibitors listed in Dataset S6. From these genes

572 that showed a characteristic expression among single-cell data, dot plots, violin plots, or feature  
573 plot visualizations were applied using Seurat functions.

574

### 575 **Comparison with *Drosophila* marker genes**

576 To check whether the *Drosophila* marker genes are applicable to shrimp, we performed a  
577 BLAST search on *the Drosophila* cell cycle and cell type markers (<https://github.com/hbc/tinyatlas>).  
578 Common genes among the three shrimp species were tblastx searched for *Drosophila*  
579 *melanogaster* genes (dmel-all-gene-r6.34.fasta; downloaded from FlyBase <https://flybase.org/>)  
580 with the parameters of e-value as 0.0001 and num\_alignments as 3.

581

### 582 **Pseudo temporal ordering of cells using Monocle 3**

583 The integrated data of Seurat were transferred to Monocle 3 (84) (<https://github.com/cole-trapnell-lab/monocle3>) to calculate a cell trajectory using the learn\_graph function. We assigned  
584 the start point based on the expression of cell proliferation-related genes and *Drosophila* marker  
585 genes of the cell cycle.

586

### 587 **Cell sorting of hemocytes and qRT-PCR of marker genes**

588 To validate the Drop-seq results on hemocytes, populations of hemocytes in the forward  
589 scatter (FSC) and side scatter (SSC) two-dimensional space were sorted using a microfluidic cell  
590 sorter (On-chip sort, On-chip Biotechnologies Co., Ltd.) from four shrimp individuals (Fig. S7). In  
591 the FSC/SSC two-dimensional space, two main populations were predicted as Region1 (R1):  
592 small/simple and Region2 (R2): large/complexity populations, which were defined as agranulocytes  
593 and granulocytes, respectively. After sorting, some sorted hemocytes were immediately fixed in 2%  
594 formalin in KPBS and stained with a May-Grunwald and Giemsa staining solution to observe the  
595 cellular components. Non-stained and stained hemocytes were subjected to microscopy IX71  
596 (Olympus Corporation) to observe their structures.

597 Total RNA was also collected from sorted cells and pre-sorted cells. The concentration of  
598 RNA was measured using a nanodrop, and cDNA was transcribed using a High-Capacity cDNA  
599 Reverse Transcription Kit (Thermo Fisher Scientific). Constructed cDNA was diluted five times with  
600 TE buffer and subjected to qRT-PCR using KOD SYBR qPCR (TOYOBO Co. Ltd.), following the  
601 manufacturer's protocol. The expression of each gene was calculated using the  $\Delta\Delta CT$  method  
602 against elongation factor-1 alpha and total hemocytes.

603

### 604 **Data files and analysis code**

605 The raw sequence data of newly sequenced *M. japonicus* transcriptomic reads were  
606 archived in the DDBJ Sequence Read Archive (DRA) of the DNA Data Bank of Japan as follows:  
607

608 MinION mRNA direct sequencing: DRA010948; Drop-seq shrimp rep1: DRA010950; shrimp rep2:  
609 DRA010951; shrimp rep3: DRA010952; mixture sample of HEK293 and 3T3 cells: DRA010949.  
610 The Seurat digital expression data were archived in the Genomic Expression Archive of the DNA  
611 Data Bank of Japan: E-GEAD-403. Fast5 data of MinION direct RNA sequencing will be made  
612 available upon request from the authors. The code used to perform *de novo* assembly, clustering,  
613 and marker analysis is available on GitHub at [https://github.com/KeiichiroKOIWA/Drop-](https://github.com/KeiichiroKOIWA/Drop-seq_on_shrimp)  
614 [seq\\_on\\_shrimp](https://github.com/KeiichiroKOIWA/Drop-seq_on_shrimp). The key resources are listed in Dataset S7.

615

## 616 **Acknowledgments**

617 We would like to thank Fumiko Sunaga for her technical support in performing cell sorting  
618 and analysis, and Editage ([www.editage.com](http://www.editage.com)) for English language editing. This work was  
619 supported by JSPS KAKENHI (JP19J00539 and JP20K15603) to K. Koiwai; a Grant-in-Aid for  
620 Scientific Research on Innovative Areas (17H06425) to K. Kikuchi.

## 621 References

- 622 1. FAO, *Fishery and aquaculture statistics 2018/FAO annuaire*, FAO yearbook (FAO, Rome, 2020).
- 623 2. P. Jiravanichpaisal, B. L. Lee, K. Söderhäll, Cell-mediated immunity in arthropods: hematopoiesis, coagulation,  
624 melanization and opsonization. *Immunobiology* **211**, 213-236 (2006).
- 625 3. A. Tassanakajon, K. Somboonwivat, P. Supungul, S. Tang, Discovery of immune molecules and their crucial  
626 functions in shrimp immunity. *Fish Shellfish Immunol* **34**, 954-967 (2013).
- 627 4. T. W. Flegel, A future vision for disease control in shrimp aquaculture. *Journal of the World Aquaculture Society*  
628 **50**, 249-266 (2019).
- 629 5. X. Zhang *et al.*, Penaeid shrimp genome provides insights into benthic adaptation and frequent molting. *Nat*  
630 *Commun* **10**, 356 (2019).
- 631 6. A. G. Bauchau, Crustaceans. *Invertebrate blood cells* **2**, 385-420 (1981).
- 632 7. K. Söderhäll, V. J. Smith, Separation of the haemocyte populations of *Carcinus maenas* and other marine  
633 decapods, and prophenoloxidase distribution. *Dev Comp Immunol* **7**, 229-239 (1983).
- 634 8. M. W. Johansson, P. Keyser, K. Sritunyalucksana, K. Söderhäll, Crustacean haemocytes and haematopoiesis.  
635 *Aquaculture* **191**, 45-52 (2000).
- 636 9. C. B. van de Braak *et al.*, The role of the haematopoietic tissue in haemocyte production and maturation in the  
637 black tiger shrimp (*Penaeus monodon*). *Fish Shellfish Immunol* **12**, 253-272 (2002).
- 638 10. M. Kondo, S. Tomonaga, Y. Takahashi, Granulocytes with cytoplasmic deposits of kuruma prawn. *Aquaculture*  
639 *Science* **60**, 151-152 (2012).
- 640 11. J. J. Dantas-Lima *et al.*, Separation of *Penaeus vannamei* haemocyte subpopulations by iodixanol density  
641 gradient centrifugation. *Aquaculture* **408-409**, 128-135 (2013).
- 642 12. J. Rodriguez, V. Boulo, E. Mialhe, E. Bachère, Characterisation of shrimp haemocytes and plasma components  
643 by monoclonal antibodies. *J Cell Sci* **108**, 1043-1050 (1995).
- 644 13. C. B. van de Braak, N. Taverne, M. H. Botterblom, W. P. van der Knaap, J. H. Rombout, Characterisation of  
645 different morphological features of black tiger shrimp (*Penaeus monodon*) haemocytes using monoclonal  
646 antibodies. *Fish Shellfish Immunol* **10**, 515-530 (2000).
- 647 14. H. H. Sung, P. Y. Wu, Y. L. Song, Characterisation of monoclonal antibodies to haemocyte subpopulations of  
648 tiger shrimp (*Penaeus monodon*): immunochemical differentiation of three major haemocyte types. *Fish*  
649 *Shellfish Immunol* **9**, 167-179 (1999).
- 650 15. H. H. Sung, R. Sun, Use of monoclonal antibodies to classify hemocyte subpopulations of tiger shrimp (*Penaeus*  
651 *monodon*). *Journal of Crustacean Biology* **22**, 337-344 (2002).
- 652 16. P. Winotaphan *et al.*, Monoclonal antibodies specific to haemocytes of black tiger prawn *Penaeus monodon*.  
653 *Fish Shellfish Immunol* **18**, 189-198 (2005).
- 654 17. Y. Lin *et al.*, Ontogenesis of haemocytes in shrimp (*Fenneropenaeus chinensis*) studied with probes of  
655 monoclonal antibody. *Dev Comp Immunol* **31**, 1073-1081 (2007).
- 656 18. J. Xing, Y. Chang, X. Tang, X. Sheng, W. Zhan, Separation of haemocyte subpopulations in shrimp  
657 *Fenneropenaeus chinensis* by immunomagnetic bead using monoclonal antibody against granulocytes. *Fish*  
658 *Shellfish Immunol* **60**, 114-118 (2017).

- 659 19. E. Z. Macosko *et al.*, Highly parallel genome-wide expression profiling of individual cells using nanoliter droplets.  
660 *Cell* **161**, 1202-1214 (2015).
- 661 20. C. Trapnell *et al.*, The dynamics and regulators of cell fate decisions are revealed by pseudotemporal ordering  
662 of single cells. *Nat Biotechnol* **32**, 381-386 (2014).
- 663 21. C. Soneson, M. D. Robinson, Bias, robustness and scalability in single-cell differential expression analysis. *Nat*  
664 *Methods* **15**, 255-261 (2018).
- 665 22. G. Raddi *et al.*, Mosquito cellular immunity at single-cell resolution. *Science* **369**, 1128-1132 (2020).
- 666 23. S. G. Tattikota *et al.*, A single-cell survey of *Drosophila* blood. *eLife* **9**, e54818 (2020).
- 667 24. S. J. Carmona *et al.*, Single-cell transcriptome analysis of fish immune cells provides insight into the evolution of  
668 vertebrate immune cell types. *Genome Res* **27**, 451-461 (2017).
- 669 25. M. S. Severo *et al.*, Unbiased classification of mosquito blood cells by single-cell genomics and high-content  
670 imaging. *Proc Natl Acad Sci U S A* **115**, E7568-E7577 (2018).
- 671 26. D. Lv *et al.*, Histone acetyltransferase KAT6A upregulates PI3K/AKT signaling through TRIM24 binding. *Cancer*  
672 *Res* **77**, 6190-6201 (2017).
- 673 27. M. Andang *et al.*, Histone H2AX-dependent GABA(A) receptor regulation of stem cell proliferation. *Nature* **451**,  
674 460-464 (2008).
- 675 28. H. C. Cheung *et al.*, Splicing factors PTBP1 and PTBP2 promote proliferation and migration of glioma cell lines.  
676 *Brain* **132**, 2277-2288 (2009).
- 677 29. M. Shibayama *et al.*, Polypyrimidine tract-binding protein is essential for early mouse development and  
678 embryonic stem cell proliferation. *FEBS J* **276**, 6658-6668 (2009).
- 679 30. H. Jiao *et al.*, TGF-beta1 Induces polypyrimidine tract-binding protein to alter fibroblasts proliferation and  
680 fibronectin deposition in keloid. *Sci Rep* **6**, 38033 (2016).
- 681 31. X. Lin, K. Söderhäll, I. Söderhäll, Transglutaminase activity in the hematopoietic tissue of a crustacean,  
682 *Pacifastacus leniusculus*, importance in hemocyte homeostasis. *BMC Immunol* **9**, 58 (2008).
- 683 32. C. C. Huang, K. Sritunyalucksana, K. Söderhäll, Y. L. Song, Molecular cloning and characterization of tiger shrimp  
684 (*Penaeus monodon*) transglutaminase. *Dev Comp Immunol* **28**, 279-294 (2004).
- 685 33. X. Lin, K. Söderhäll, I. Söderhäll, Invertebrate hematopoiesis: an astakine-dependent novel hematopoietic factor.  
686 *J Immunol* **186**, 2073-2079 (2011).
- 687 34. J. Huerta-Cepas *et al.*, eggNOG 5.0: a hierarchical, functionally and phylogenetically annotated orthology  
688 resource based on 5090 organisms and 2502 viruses. *Nucleic Acids Res* **47**, D309-D314 (2019).
- 689 35. J. Huerta-Cepas *et al.*, Fast genome-wide functional annotation through orthology assignment by eggNOG-  
690 Mapper. *Mol Biol Evol* **34**, 2115-2122 (2017).
- 691 36. I. Söderhäll, Crustacean hematopoiesis. *Dev Comp Immunol* **58**, 129-141 (2016).
- 692 37. F. De Lucia, J. Q. Ni, C. Vaillant, F. L. Sun, HP1 modulates the transcription of cell-cycle regulators in *Drosophila*  
693 *melanogaster*. *Nucleic Acids Res* **33**, 2852-2858 (2005).
- 694 38. R. Paro, D. S. Hogness, The polycomb protein shares a homologous domain with a heterochromatin-associated  
695 protein of *Drosophila*. *Proc Natl Acad Sci U S A* **88**, 263-267 (1991).



- 696 39. M. Mohan *et al.*, The *Drosophila* insulator proteins CTCF and CP190 link enhancer blocking to body patterning.  
697 *EMBO J* **26**, 4203-4214 (2007).
- 698 40. J. E. Rasko *et al.*, Cell growth inhibition by the multifunctional multivalent zinc-finger factor CTCF. *Cancer Res*  
699 **61**, 6002-6007 (2001).
- 700 41. C. L. Scott *et al.*, Role of the chromobox protein CBX7 in lymphomagenesis. *Proc Natl Acad Sci U S A* **104**, 5389-  
701 5394 (2007).
- 702 42. K. Junkunlo, K. Söderhäll, C. Noonin, I. Söderhäll, PDGF/VEGF-related receptor affects transglutaminase activity  
703 to control cell migration during crustacean hematopoiesis. *Stem Cells Dev* **26**, 1449-1459 (2017).
- 704 43. X. Lin, I. Söderhäll, Crustacean hematopoiesis and the astakine cytokines. *Blood* **117**, 6417-6424 (2011).
- 705 44. C. Noonin, X. Lin, P. Jiravanichpaisal, K. Söderhäll, I. Söderhäll, Invertebrate hematopoiesis: an anterior  
706 proliferation center as a link between the hematopoietic tissue and the brain. *Stem Cells Dev* **21**, 3173-3186  
707 (2012).
- 708 45. N. D. Leigh *et al.*, von Willebrand factor D and EGF domains is an evolutionarily conserved and required feature  
709 of blastemas capable of multitissue appendage regeneration. *Evol Dev* **22**, 297-311 (2020).
- 710 46. L. J. Brown *et al.*, Lipocalin-7 is a matricellular regulator of angiogenesis. *PLoS One* **5**, e13905 (2010).
- 711 47. S. Mary, M. J. Kulkarni, S. S. Mehendale, S. R. Joshi, A. P. Giri, Tubulointerstitial nephritis antigen-like 1 protein  
712 is downregulated in the placenta of pre-eclamptic women. *Clin Proteomics* **14**, 8 (2017).
- 713 48. M. Shen *et al.*, Tinag1 suppresses triple-negative breast cancer progression and metastasis by simultaneously  
714 inhibiting integrin/FAK and EGFR signaling. *Cancer Cell* **35**, 64-80 (2019).
- 715 49. G. Neufeld, T. Cohen, S. Gengrinovitch, Z. Poltorak, Vascular endothelial growth factor (VEGF) and its receptors.  
716 *The FASEB Journal* **13**, 9-22 (1999).
- 717 50. M. Peichev *et al.*, Expression of VEGFR-2 and AC133 by circulating human CD34(+) cells identifies a population  
718 of functional endothelial precursors. *Blood* **95**, 952-958 (2000).
- 719 51. A. I. Munier *et al.*, PVF2, a PDGF/VEGF-like growth factor, induces hemocyte proliferation in *Drosophila* larvae.  
720 *EMBO Rep* **3**, 1195-1200 (2002).
- 721 52. S. Varma Shrivastav, A. Bhardwaj, K. A. Pathak, A. Shrivastav, Insulin-like growth factor binding protein-3 (IGFBP-  
722 3): unraveling the role in mediating IGF-independent effects within the cell. *Front Cell Dev Biol* **8**, 286 (2020).
- 723 53. J. Castillo, M. R. Brown, M. R. Strand, Blood feeding and insulin-like peptide 3 stimulate proliferation of  
724 hemocytes in the mosquito *Aedes aegypti*. *PLoS Pathog* **7**, e1002274 (2011).
- 725 54. G. Wang *et al.*, IGFBP7 promotes hemocyte proliferation in small abalone *Haliotis diversicolor*, proved by dsRNA  
726 and cap mRNA exposure. *Gene* **571**, 65-70 (2015).
- 727 55. W. Charoensapsri *et al.*, Laminin receptor protein is implicated in hemocyte homeostasis for the whiteleg  
728 shrimp *Penaeus (Litopenaeus) vannamei*. *Dev Comp Immunol* **51**, 39-47 (2015).
- 729 56. R. D. Rosa, M. A. Barracco, Antimicrobial peptides in crustaceans. *Isj-Invert Surviv J* **7**, 262-284 (2010).
- 730 57. E. Bachère *et al.*, Insights into the anti-microbial defense of marine invertebrates: the penaeid shrimps and the  
731 oyster *Crassostrea gigas*. *Immunol Rev* **198**, 149-168 (2004).
- 732 58. K. Y. Chen *et al.*, *Penaeus monodon* chitin-binding protein (PmCBP) is involved in white spot syndrome virus  
733 (WSSV) infection. *Fish Shellfish Immunol* **27**, 460-465 (2009).

- 734 59. S. Elbahnaswy *et al.*, A novel viral responsive protein (MjVRP) from *Marsupenaeus japonicus* haemocytes is  
735 involved in white spot syndrome virus infection. *Fish Shellfish Immunol* **70**, 638-647 (2017).
- 736 60. M. Munoz, F. Vandenbulcke, D. Saulnier, E. Bachère, Expression and distribution of penaeidin antimicrobial  
737 peptides are regulated by haemocyte reactions in microbial challenged shrimp. *Eur J Biochem* **269**, 2678-2689  
738 (2002).
- 739 61. K. Zhang, K. Koiwai, H. Kondo, I. Hirono, White spot syndrome virus (WSSV) suppresses penaeidin expression in  
740 *Marsupenaeus japonicus* hemocytes. *Fish & Shellfish Immunol* **78**, 233-237 (2018).
- 741 62. S. Li, Z. Wang, F. Li, K. Yu, J. Xiang, A novel vascular endothelial growth factor receptor participates in white spot  
742 syndrome virus infection in *Litopenaeus vannamei*. *Front Immunol* **8**, 1457 (2017).
- 743 63. Z. Wang, S. Li, F. Li, S. Xie, J. Xiang, Identification and function analysis of a novel vascular endothelial growth  
744 factor, LvVEGF3, in the Pacific whiteleg shrimp *Litopenaeus vannamei*. *Dev Comp Immunol* **63**, 111-120 (2016).
- 745 64. Z. Wang *et al.*, Identification and characterization of two novel vascular endothelial growth factor genes in  
746 *Litopenaeus vannamei*. *Fish Shellfish Immunol* **84**, 259-268 (2019).
- 747 65. R. D. Rosa *et al.*, Functional divergence in shrimp anti-lipopolysaccharide factors (ALFs): from recognition of cell  
748 wall components to antimicrobial activity. *PLoS One* **8**, e67937 (2013).
- 749 66. I. Söderhäll, Recent advances in crayfish hematopoietic stem cell culture: a model for studies of hemocyte  
750 differentiation and immunity. *Cytotechnology* **65**, 691-695 (2013).
- 751 67. H. N. Mai, H. T. Nguyen, K. Koiwai, H. Kondo, I. Hirono, Characterization of a Kunitz-type protease inhibitor  
752 (MjKuPI) reveals the involvement of MjKuPI positive hemocytes in the immune responses of kuruma shrimp  
753 *Marsupenaeus japonicus*. *Dev Comp Immunol* **63**, 121-127 (2016).
- 754 68. K. Koiwai *et al.*, Two hemocyte sub-populations of kuruma shrimp *Marsupenaeus japonicus*. *Mol Immunol* **85**,  
755 1-8 (2017).
- 756 69. K. Koiwai, H. Kondo, I. Hirono, Isolation and molecular characterization of hemocyte sub-populations in kuruma  
757 shrimp *Marsupenaeus japonicus*. *Fisheries Science* **85**, 521-532 (2019).
- 758 70. T. Sequeira, D. Tavares, M. Arala-Chaves, Evidence for circulating hemocyte proliferation in the shrimp *Penaeus*  
759 *japonicus*. *Dev Comp Immunol* **20**, 97-104 (1996).
- 760 71. O. Rota-Stabelli, A. C. Daley, D. Pisani, Molecular timetrees reveal a Cambrian colonization of land and a new  
761 scenario for ecdysozoan evolution. *Curr Biol* **23**, 392-398 (2013).
- 762 72. G. W. C. Thomas *et al.*, Gene content evolution in the arthropods. *Genome Biol* **21**, 15 (2020).
- 763 73. J. M. Wolfe *et al.*, A phylogenomic framework, evolutionary timeline and genomic resources for comparative  
764 studies of decapod crustaceans. *Proc Biol Sci* **286**, 20190079 (2019).
- 765 74. L. Broseus *et al.*, TALC: Transcript-level Aware Long-read Correction. *Bioinformatics*  
766 10.1093/bioinformatics/btaa634 (2020).
- 767 75. E. Bushmanova, D. Antipov, A. Lapidus, A. D. Prjibelski, rnaSPAdes: a *de novo* transcriptome assembler and its  
768 application to RNA-Seq data. *Gigascience* **8**, 1-13 (2019).
- 769 76. M. G. Grabherr *et al.*, Full-length transcriptome assembly from RNA-Seq data without a reference genome. *Nat*  
770 *Biotechnol* **29**, 644-652 (2011).

- 771 77. M. Biočanin, J. Bues, R. Dainese, E. Amstad, B. Deplancke, Simplified Drop-seq workflow with minimized bead  
772 loss using a bead capture and processing microfluidic chip. *Lab Chip* **19**, 1610-1620 (2019).
- 773 78. S. Picelli *et al.*, Tn5 transposase and tagmentation procedures for massively scaled sequencing projects. *Genome*  
774 *Research* **24**, 2033-2040 (2014).
- 775 79. B. Langmead, S. L. Salzberg, Fast gapped-read alignment with Bowtie 2. *Nat Methods* **9**, 357-359 (2012).
- 776 80. A. Butler, P. Hoffman, P. Smibert, E. Papalexi, R. Satija, Integrating single-cell transcriptomic data across  
777 different conditions, technologies, and species. *Nat Biotechnol* **36**, 411-420 (2018).
- 778 81. C. Hafemeister, R. Satija, Normalization and variance stabilization of single-cell RNA-seq data using regularized  
779 negative binomial regression. *Genome Biol* **20**, 296 (2019).
- 780 82. C. Camacho *et al.*, BLAST+: architecture and applications. *BMC Bioinformatics* **10**, 421 (2009).
- 781 83. S. F. Altschul, W. Gish, W. Miller, E. W. Myers, D. J. Lipman, Basic local alignment search tool. *Journal of*  
782 *Molecular Biology* **215**, 403-410 (1990).
- 783 84. J. Cao *et al.*, The single-cell transcriptional landscape of mammalian organogenesis. *Nature* **566**, 496-502 (2019)